Abstract

Photodynamic therapy suppresses tumor growth in an Animal Model of Human Infantile Hemangioma

Woo Jung Kim
College of Medicine, Plastic Surgery
The Graduate School
Seoul National University

Purpose: The author investigated the efficacy of photodynamic therapy against infantile hemangiomas using the hemangioma animal model.

Materials and Methods: Eighty-three hemangioma specimens from 5 children were implanted into nude mice. The gross and volume changes of the implants were evaluated for up to 13 weeks. The histological change of the implant was evaluated at 5 weeks after transplantation. Photodynamic therapy was performed between 6 and 10 weeks after transplantation. The photosensitizer uptake of the implant was evaluated at 24 hours after photosensitizer administration. The implant response was evaluated at 0, 12, and 24 hours after light delivery. The change in ATF3 levels, a transcription factor induced under severe hypoxic conditions, were investigated immediately after treatment.

Results: The implant's volume increased slowly during the first 4 weeks and then became involuted. At 5 weeks after transplantation, plump endothelial cells formed tightly packed sinusoidal channels, and the endothelial cells were positive for CD31 and GLUT1 expression. At 24 hours after photosensitizer administration, confocal analysis showed that photosensitizer was present within CD31-positive cells. The implant volume was significantly decreased in the treated implants compared with the untreated implants ($p < .0001$). At 24 hours after light delivery, most cells had collapsed. ATF3 expression increased gradually and then reached a maximum level at 4 hours after treatment.

Conclusion: Photodynamic therapy was effective in the treatment for infantile hemangiomas.

Apoptosis, a major mechanism of hemangioma destruction in the early phase, might be caused by ischemic injury as well as direct effects of photodynamic therapy.

Key words: Photodynamic therapy, Hemangioma animal model, Photofrin, GLUT1, ATF3, Endothelial cell

Student number: 2005-30606

List of Tables

Table 1. Demographics of Patients with Juvenile Hemangioma 10

List of Figures

Figure 1. A flow diagram presenting the progress of the study……11

Figure 2. Volume change with time after transplantation in hemangioma animal model...……12

Figure 3. Histological finding at 5 weeks after transplantation…….……..……..…13

Figure 4. Confocal micrographs at 24 hours after Photofrin administration…….……..…14

Figure5. Volume change with times after PDT…….……..……...…..……15

Figure6. Implant response to PDT at 2 weeks after PDT.……...…..……16

Figure7. Histological finding of implants after PDT……...…….……17

Figure8. Expression of ATF3 at 0, 1, 2, 4, and 12 hours after PDT……18

List

Introduction 1

Purpose.....2

Materials and Methods.....3

Results.....7

Legends.....10

Discussion.....19

Conclusion.....23

References.....24

Abstract.....27

Introduction

Infantile hemangiomas are the most common tumor of infancy and childhood, occurring in 1% to 3% of all neonates.[1,2] Because most hemangiomas are small and harmless tumors and result in a spontaneous resolution, they do not need treatment. However, some hemangiomas can cause several clinical problems, such as a mass effect on surrounding facial features, bleeding, deep ulceration, and secondary infection. These cases require immediate treatment, including pharmacological therapy, such as steroids and interferon alpha, and operative management. However, these treatments can cause various local and systemic side effects, such as cushingoid face, scars, and rarely, spastic diplegia[3].

Photodynamic therapy (PDT) is a noninvasive method in which a photosensitizer and light source are used. As a type of targeted therapy, PDT does not have systemic side effects such as those that occur with systemic corticosteroid therapy or interferon alpha therapy. When simple excision of the hemangioma is impossible or severe postoperative complications are expected, PDT can be considered as an alternative treatment.

Previously an animal model of infantile hemangioma using experimentally induced angiosarcoma to investigate the therapeutic effects of PDT on hemangioma was reported.[4] However, although angiosarcoma has some histological features similar to hemangioma, it does not follow the characteristic clinical course of hemangioma, which show rapid growth, slow regression, and no recurrence. Recently, a novel model of infantile hemangioma was established using xenografts of human hemangioma tissue in nude mice.[5] This model imitated the natural course of infantile hemangioma, and the chief cellular components were endothelial cells of human origin.

Purpose

The purpose of this study is to evaluate the effect of photodynamic therapy (PDT) against human infantile hemangioma and its mechanism, using an experimental model of xenografted human infantile hemangioma. In addition, we developed in vivo an animal model of human infantile hemangioma.

Material and methods

1. Animal Model

All experiments in this study were performed in accordance with the guidelines for animal research from the National Institutes of Health and approved by the Institutional Animal Care and Use Committee and institutional review board at Seoul National University Hospital in Seoul, Korea (11-0342, H-1003-002-310). Five children with proliferative hemangioma were included in this study between May 2010 and February 2012 (Table 1). Because of distress to their caretakers, the hemangiomas were excised by a simple excision. As proposed by Tang et al,[5] the cutaneous portion and fibrofatty tissue surrounding the specimen were removed, and the remainder was cut into small pieces of approximately 5 × 4 × 3 mm. Twenty pieces from patient 1, 19 pieces from patient 2, 18 pieces from patient 3, 11 pieces from patient 4, and 15 pieces from patient 5 were obtained. Athymic nude mouse (Orient Co. Ltd, Seoul, Korea) at six weeks of age was subcutaneously implanted with the tumor pieces, with 4 each in the back. Because the experiment was conducted in five times, a total of 22 athymic nude mice was used. Anesthesia was performed through intramuscular injection with zolazepam (5 mg/kg, Zoletil®, Virbac, Carros, France) and xylazine (10 mg/kg, Rompun®, Bayer Korea, Seoul, Korea).

The implants of patients 1, 2, 3, 4, and 5 were used to evaluate the gross change and implant volume change up to 13 weeks. The specimens were harvested at a given time for histological examinations and protein assays (patient 1 for evaluating the histological change of the implant after xenografting, patient 3 for evaluating the photosensitizer uptake of the implant, and patients 4 and 5 for evaluating the implant response to PDT and the underlying mechanism) (Fig. 1).

2. Morphometry

To identify whether the implant followed the natural course of infantile hemangioma, changes in the gross appearance and implant volume were assessed once per week up to 4 weeks and once every 3 weeks thereafter up to 13 weeks. To calculate the implant volume, the maximal length (a) of implants

and the perpendicular length (*b*) were measured with a sliding caliper. The volume (*V)* of implants was estimated as $V = \pi/6 \times a \times b^{2}$.[6] Implant volume change was expressed as a percentage of the implant volume estimated at one week after transplantation.

3. Histology

To identify whether the histology of the implant resembled infantile hemangioma, at 5 weeks after transplantation, specimens harvested from the implants of patient 1 were formalin fixed, paraffin embedded, 4-μm sectioned, and stained with hematoxylin and eosin. GLUT1 and CD31 immunostaining was also performed. Briefly, deparaffinized sections were microwaved for 10 minutes and blocked with 2% skim milk. The sections were then incubated with the primary antibodies against human CD31 (Abcam, Cambridge, USA) at a 1:100 dilution for 2 hours and GLUT1 (Abcam, Cambridge, USA) at a 1:100 dilution for 1 hour. Subsequently, the sections were incubated with secondary antibody at 1:200 for 1 hour. CD31 and GLUT1 immunolabeling was detected using DAB and counterstained using Mayer's hematoxylin.

4. Photosensitizer and Light Sources

Between 6 and 10 weeks after transplantation**,** Photofrin (Axcan Pharma Inc., Quebec, Canada) was dissolved in phosphate-buffered saline at a concentration of 1 mg/ml and injected through the tail vein at a dose of 5 mg/kg. At 24 hours after administration, light was delivered using a diode laser (CeramOptec GMBH, Bonn, Germany) at 630 nm with a fluence rate of 150 mW/cm^2 and a dose of 100 J/cm^2 for an irradiation time of 667 s. Because red light with a wavelength of 630 nm does not penetrate deeply into the skin,[7] a subcutaneous tunnel was created with minimal dissection around the implant, and an optical fiber was placed in the tunnel to allow the light to penetrate into the entire implant despite its subcutaneous position.

5. Evaluation of Photosensitizer Uptake in Implant

At 24 hours after Photofrin administration and before light delivery, the specimens were formalin

fixed and paraffin embedded. Sections (4-µm thick) were deparaffinized in xylene and dehydrated with a sequential ethanol gradient. Antigen retrieval was carried out by heating the sections in citrate-EDTA buffer (10 mM citric acid, 2 mM EDTA, and 0.05% Tween-20, pH 6.2) or Tris-EDTA buffer (10 mM Trizma base, 1 mM EDTA, and 0.05% Tween-20, pH 9). The sections were blocked for 1 hour in 5% serum and incubated with fluorescein isothiocyanate (FITC)–labeled mouse antihuman CD31 monoclonal antibody (dilution, 1:500; BD Bioscience, San Jose, Calif., USA). The sections were washed and blocked again for 30 minutes. The sections were counterstained with 4', 6-diamidino-2-phenylindole(DAPI**;** Molecular Probes, Eugene, OR, USA),mounted with the ProLong Antifade Kit (Molecular Probes, Eugene, OR, USA) and observed under a confocal microscope (Bio-Rad MRC-1042 MP; BioRad, Hemel Hempstead, United Kingdom). The sections were imaged for Photofrin (excitation 635 nm) and CD31 staining (excitation 490 nm).

6. Evaluation of Implant Response

a. morphometry

On days 2, 6, and 14 after light delivery, gross evaluation and implant volume change were assessed as mentioned above. Changes in implant volume were expressed as a percentage of the implant volume estimated immediately before light delivery.

b. histology

The specimens, harvested from the implants of patient 4 and 5 at 0, 12, 24 hours after light delivery were formalin-fixed, paraffin-embedded, 4-micrometer-sectioned. H&E and CD31 immunostaining were done as mentioned above. TUNEL staining was performed using the ApopTag (Intergen Company, Norcross, Georgia). Briefly, the tissue specimens were deparaffinized and then pretreated with a protein digesting enzyme followed by endogenous peroxidase quenching. A working strength TdT (terminal deoxynucleotidyltransferase) enzyme was then applied to the specimen followed by application of anti-digoxigenin conjugate. Color was developed inperoxidase substrate and after appropriate washing a counterstain with 0.5% methyl green was applied. After appropriate dehydration the specimens were mounted and covered with a glass coverslip and observed with the

light microscope.

c. ATF3 western blotting

The specimens, harvested from the implants of patient 5 at 0, 1, 2, 4, 12 hours after light delivery were homogenized in a protein extraction solution (RIPA buffer; Cell Signaling Technology, MA, USA) using polytron homogenizer (Fisher Scientific, PA, USA). The protein content was measured using a Bio-Rad colorimetric protein assay kit (Bio-Rad, CA, USA). A 20 ug sample of the protein was separated on sodium dodecyl sulfate (SDS)-polyacrylamide gels and transferred onto a nitrocellulose membrane (Invitrogen, CA, USA). Activating transcription factor-3 (ATF3) (1:1000,Abcam, Cambridge, UK) and mouse monoclonal anti-beta-actin (1:5000, Santa Cruz Biotechnology Inc, CA, USA) antibodies were used a primary antibody and horseradish peroxidase-conjugated antibody (1:5000,KPL, MD, USA) was used as a secondary antibody. Band detection was performed using the enhanced chemiluminescence (ECL) detection system (Amersham Pharmacia Biotech). Image and quantification acquired using a FluorChem HD2 system (protein simple, California, USA). The density of each ATF3 band was normalized against that of beta actin.

Statistical evaluations

Implant response was assessed by comparing implant volume change at 2 weeks after light delivery with the change of untreated implant in Patient 2 and 3. Additionally, the response of the implants from each patient and individual differences in volume were assessed. The data were analyzed with analysis of covariance (ANCOVA). *P* values <0.05 were considered as statistically significant.

Results

1. Reproducibility of the Animal Model of Infantile Hemangiomas

Six implants (2 implants of patient 1, 1 implant of patient 2,and 3 implants of patient 5) that had ulcer or perforation on the overlying skin were excluded. The changes in gross appearance and implant volume were assessed in a total of 34 implants (16 implants of patient 1, 7 implants of patient 2, 6 implants of patient 3, 3 implants of patient 4, and 2 implants of patient 5) for up to 13 weeks. According to the volume change curves of each donor patient implant, all implants but those from patient 2 grew during the first 4 weeks and then involuted (Figure 2, left). However, the times when the implants began to grow and achieved their maximum volume were differed among the patients. In total, most of the implant demonstrated a slow volume increase to approximately 132.9% during the first4 weeks, a rapid decrease to approximately 50.8% over the next 3 weeks, and then slow involution. At the final observation (13 weeks), the volume remained at 12.0% (Figure 2, right). At 5 weeks after transplantation, light microscopy showed that plump endothelial cells formed tightly packed sinusoidal channels (Figure 3, above). Immunohistochemical staining showed that the endothelial cells were positive for CD31 and GLUT1 expression (Figure 3, below). All these histological features resembled typical infantile hemangiomas in the proliferative phase.

2. Effective Uptake of Photosensitizer

At 24 hours after Photofrin administration and before light delivery, confocal analysis showed that Photofrin was present within the CD31-positive cells (Figure 4). Photofrin effectively accumulated within endothelial cells, which are the major component of infantile hemangiomas.

3. Significant Response to PDT

PDT was performed in total 41 implants (11 implants of patient 2, 12 implants of patient 3, 8 implants of patient 4 and 10 implants of patient 5). Excluding implants used for biopsy specimens, changes in the gross appearance and implant volume were assessed for up to 2 weeks after light

delivery in a total of 27 implants (11 implants from patient 2, 10 implants from patient 3, 4 implants from patient 4 and 2 implants from patient 5). Within 2 weeks, 3 implants from patient 3 and 2 implants from patient 4 disappeared, leaving an ulcer with or without an erythematous border. On days 2, 6, and 14, the implant volume decreased by approximately 21.6%, 49.6%, and 72.6%, respectively, of the volume estimated immediately before light delivery (Figure 5). The rate of decrease was gradually reduced during observation. To evaluate the implant response to PDT, we compared the implant volume change at 2 weeks after light delivery with the change of untreated implant. For the implants from patient 2, the implant volume was significantly decreased in the treated implants compared with the untreated implants ($p< .0001$). For the implants from patient 3, the implant volume was significantly decreased in the treated implants compared with the untreated implants ($p= .007$). In total, the implant volume was significantly decreased in the treated implants compared with the untreated implants ($p< .0001$) (Figure 6).The decrease in implant volume after light delivery was not significantly different between patient 2 and patient 3 ($p=.2838$).

Before PDT, histological examination showed a mass composed of immature capillaries with tiny lumens lined by plump endothelial cells with an outer concentric pericyte layer (Figure 7, above left). The endothelial lining of microvessels was observed with CD31 immunostaining (Figure 7, middle left). Apoptotic cells were sporadically observed (Figure 7, below left). At 12 hours after light delivery, few inflammatory cells were observed in the intravascular spaces or an intrinsic part of the implant, and the extravasation of red blood cells with dilatation of vascular structure was observed (Figure 7, above center). CD31 immunostaining showed a disruption of the endothelial lining and a marked decrease in CD31 expression (Figure 7, middle center). A significant amount of apoptotic cells were diffusely distributed (Figure 7, below center). At 24 hours after light delivery, most cells had collapsed, and marked neutrophil and lymphocyte infiltration was observed (Figure 7, above right). CD31-positive cells and apoptotic cell death were rarely observed (Figure 7, middle right and below right).

4. Hypoxia-Induced ATF3 Expression

We investigated the change in ATF3 levels immediately after PDT (< 12 hours). ATF3 expression increased gradually and then reached a maximum level at 4 hours after PDT, which was approximately 2-fold over baseline as assessed by densitometric analysis. At 12 hours after PDT, ATF3 expression decreased (Figure 8).

Legends

Table 1. Demographics of Patients with Juvenile Hemangioma

Patient	Age (month)	Sex	Location
1	6	M	Right eyebrow
2	10	F	Forehead
3	10	F	Left forearm
4	9	F	Posterior neck
5	9	M	Right eyebrow

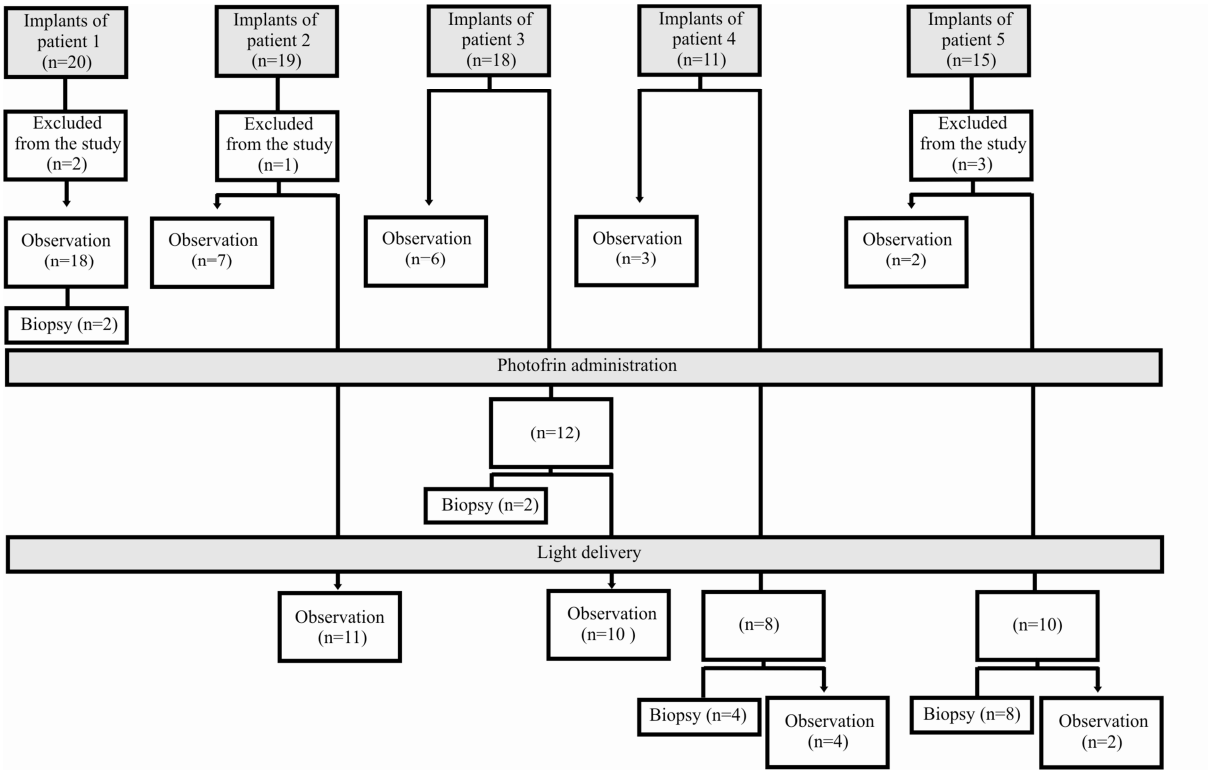

Figure 1. A flow diagram presenting the progress of the study. The 6 implants which had ulcer or perforation on the overlying skin were excluded. A total of 36 implants were used for checking reproducibility of the animal model of infantile hemangiomas. A total of 41 implants were used for evaluating the efficacy of PDT against infantile hemangiomas.

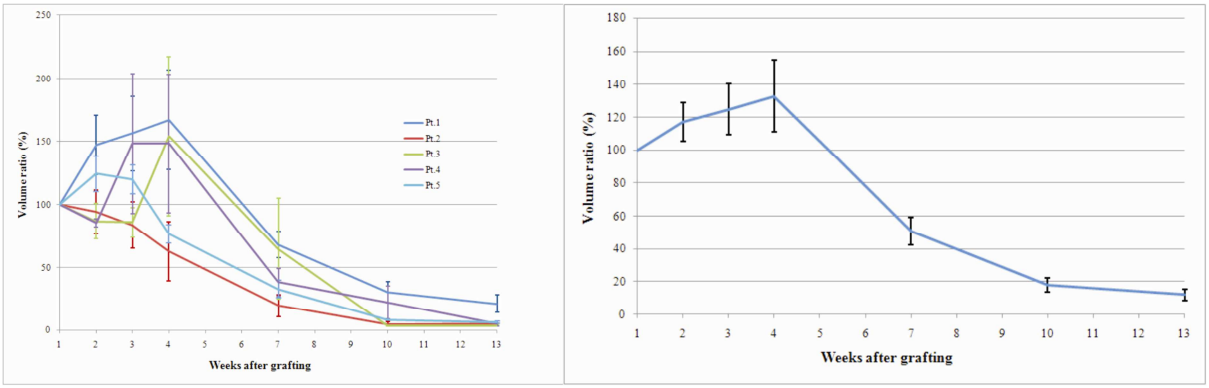

Figure 2. Volume change with time after transplantation in hemangioma animal model. Implant volume change was expressed as a percentage of the implant volume estimated at one week after transplantation. Results are expressed as mean ± SE. (Left) Volume change according to each donor patient of hemangioma xenogaft. (Right) Mean volume change of all 5 donor patients.

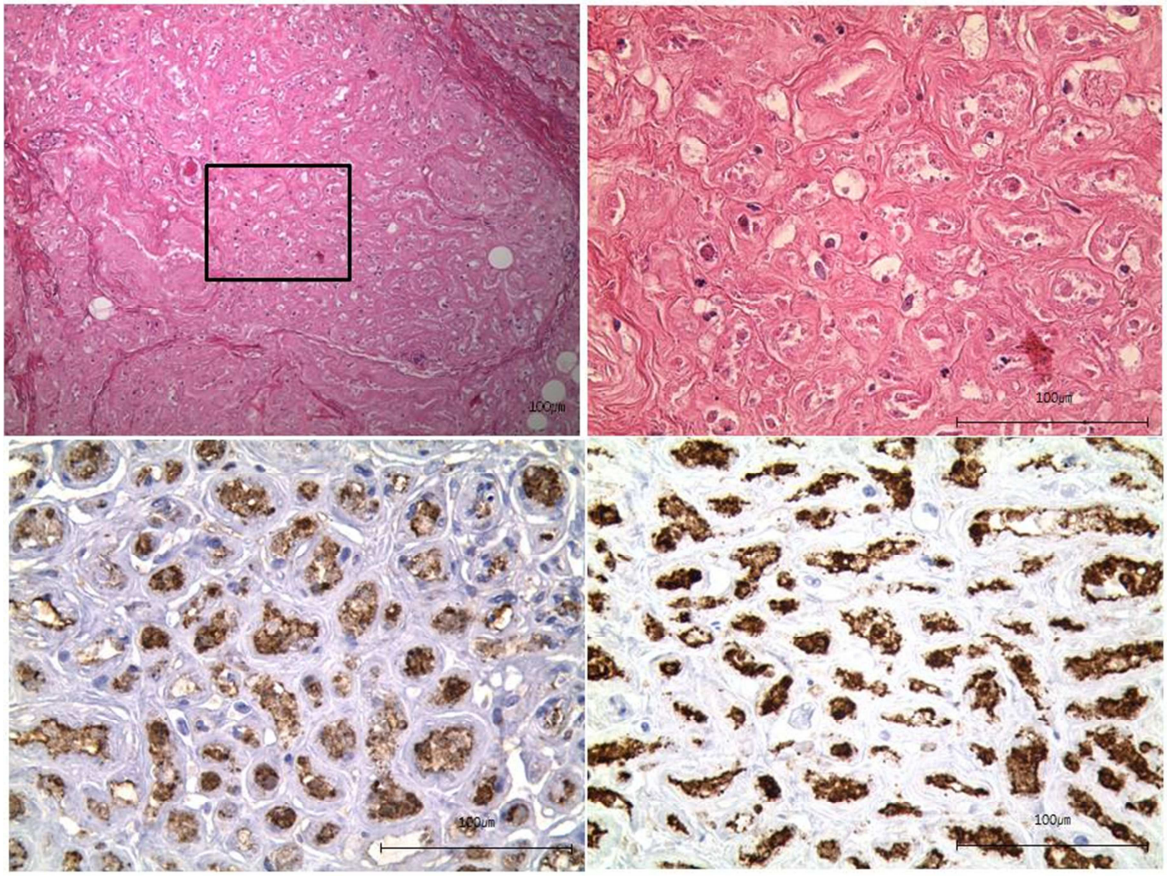

Figure 3. Histological finding at 5 weeks after transplantation. (Above) Hematoxylin and eosin staining showed that plump endothelial cells formed tightly packed sinusoidal channels, and karyogenesis was frequent in implant. Immunohistochemical staining showed that the endothelial cells were positive for GLUT-1 (below left) and CD31 (below right) expression. All these histological features resembled typical infantile hemangiomas in the proliferative phase. Magnification; above left, x100; the others, x400.

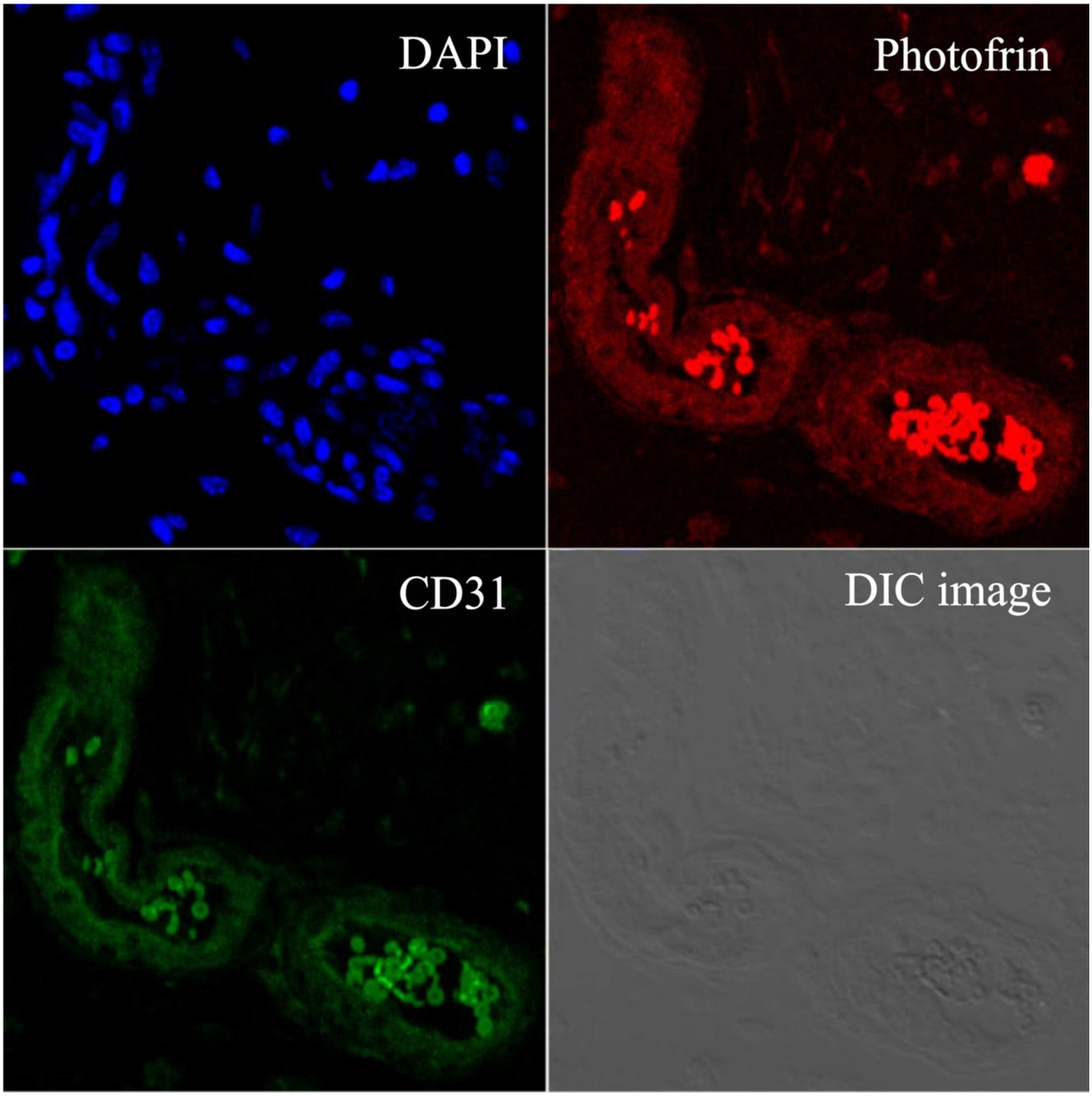

Figure 4. Confocal micrographs at 24 hours after Photofrin administration. Photofrin fluorescence (above right) and CD31 staining (below left) in the same region were observed. The confocal analysis showed that Photofrin was present within the CD31-positive cells. They meant that an effective accumulation of Photofrin in the endothelial cell, which was major component of infantile hemangiomas (magnification, x600).

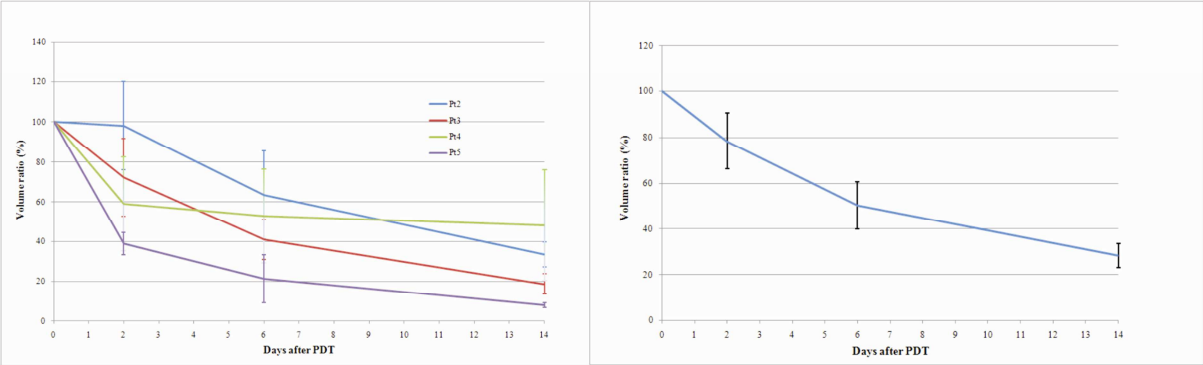

Figure 5. Volume change with times after PDT. Implant volume change was expressed as a percentage of the implant volume estimated immediately before light delivery. Results are expressed as mean ± SE. (Left) Volume change according to each donor patient of hemangioma xenogaft. (Right) Total volume change.

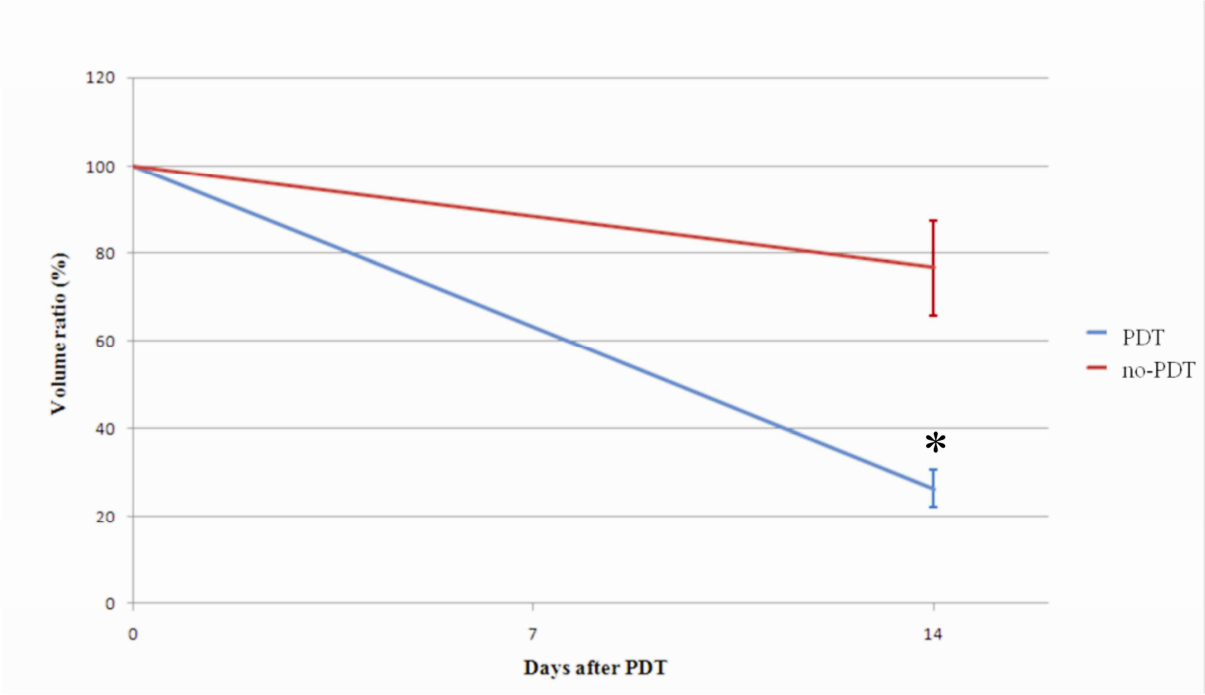

Figure 6. Implant response to PDT at 2 weeks after PDT. Results are expressed as mean ± SE. The implant volume was significantly decreased in the PDT-treated implants compared with the untreated implants. *, $p < 0.05$.

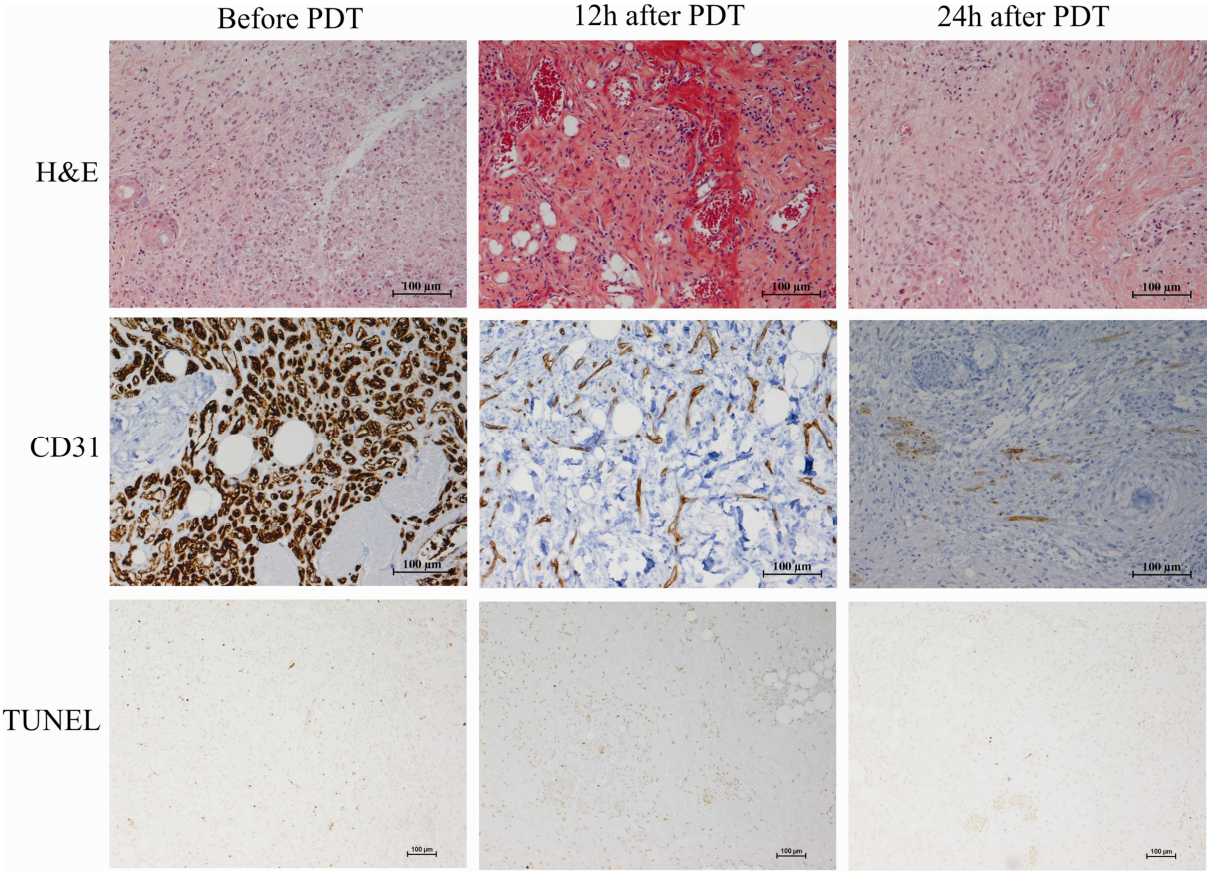

Figure 7. Histological finding of implants after PDT. Before PDT, Hematoxylin and eosin staining (above left) showed a mass composed of immature capillaries with tiny lumens lined by plump endothelial cells with an outer concentric pericyte layer. At CD31 immunostaining(middle left), the endothelial lining of microvessel was observed. At TUNEL staining (below left), apoptotic cells were found sporadically. At 12 hours after light delivery, scarce inflammatory cells were seen in the intravascular spaces and an intrinsic part of the implant, and extravasation of red blood cells with dilatation of vascular structure was observed in H&E stain (above center). CD31 immunostaining (middle center) showed a disruption of the endothelial lining, and had a marked decrease in expression. A significant amount of apoptotic cells were distributed diffusely (below center). At 24 hours after light delivery, most cells had collapsed, and marked infiltration of neutrophils and lymphocytes was observed (above right). CD31 staining cells and apoptotic cell death were almost not observed (middle right and below right).

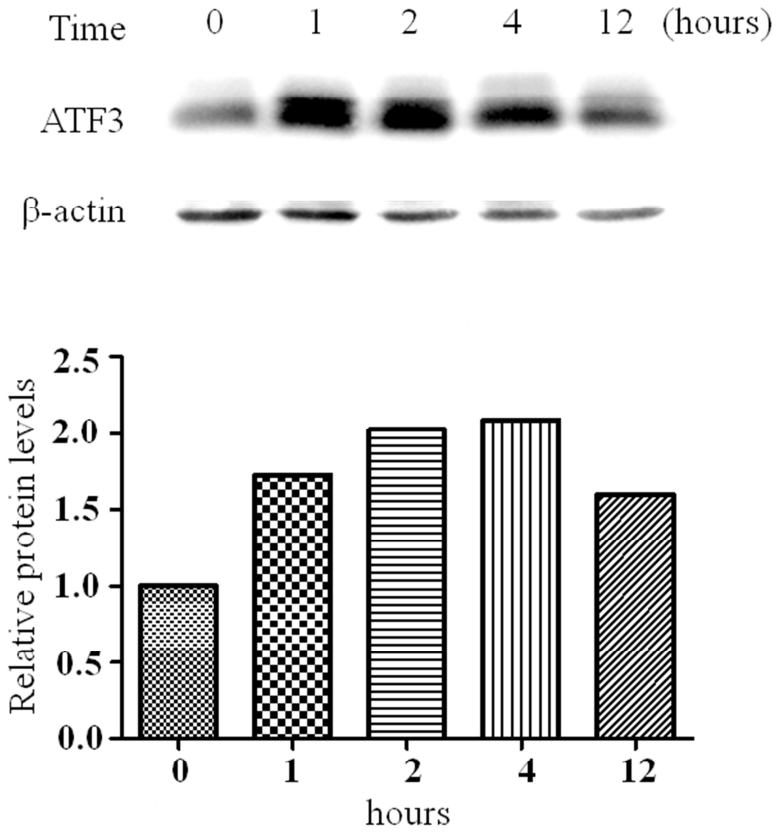

Figure 8. Expression of ATF3 at 0, 1, 2, 4, and 12 hours after PDT. ATF3 expression increased gradually and then reached a maximum level at 4 hours after PDT, which was approximately 2-fold over that of the baseline. At 12 hours after PDT, ATF3 expression decreased. They meant that in 12 hours after PDT, ATF3-mediated pathway, which was involved in ischemia-induced apoptosis was activated.

Discussion

After xenografts of human hemangioma tissue were established in nude mice, we evaluated changes in the gross appearance and implant volume in 34 implants. Histological examinations were performed using H&E, CD31 immunostaining, and GLUT1 immunostaining. GLUT1, an erythrocyte-type glucose transport protein, is a highly specific immunohistochemical marker for infantile hemangiomas[8] and is useful for an extra diagnostic tool to differentiate between hemangiomas and vascular malformations.[9] Most of our implants grew during the first 4 weeks and then became involuted. However, they did not grow rapidly, and the maximum volume (140.7%) was much smaller than those of Tang et al[5] (>200%). Additionally, they regressed relatively rapidly, unlike the results of Tang et al.[5] However, histological examinations before PDT showed that plump endothelial cells formed tightly packed sinusoidal channels, and the endothelial cells highly expressed both CD31 and GLUT1(Fig.7). These histological features were identical to those of typical infantile hemangiomas in the proliferative phase. Tang et al,[5]before rapid growth, demonstrated a brief period of shrinkage, and the authors explained that it was caused by ischemic damage that developed in the central area during implant revascularization. The growth of our implants was irregular, which might be due to irreversible ischemic damage caused by delayed revascularization despite minimal dissection and a short time interval between graft harvest and implantation (within 30 minutes). Scattered localizations of fibrofatty tissues, evidences of irreversible ischemic injury, were observed in our implants.

Photofrin, which is used in this study, is one of the most common clinically used photosensitizer. For PDT using Photofrin to be effective in the treatment of infantile hemangiomas, the injected Photofrin should not be confined within the blood vessels but should be selectively taken up by vascular endothelial cells because hemangiomas are composed of tightly packed sinusoidal channels lined by mitotically active endothelial cells and pericytes. At 24 hours after Photofrin administration, confocal analysis showed that Photofrin was present within the CD31-positive endothelial cells, which demonstrated an effective accumulation of Photofrin in the intrinsic parts of hemangiomas. Leuning et al.[10] noted that vascular endothelial cells incorporated more Photofrin than mouse

fibroblasts and amelanotic hamster melanoma cells.

Because clinical problems requiring immediate treatment, such as ulceration and bleeding are common during the proliferating phase of hemangioma[11] and this is the period in which it is histopathologically most proliferative, PDT was performed on implants between 6 and 10 weeks after transplantation, when the implants had histological features identical to the proliferative phase of infantile hemangioma. The dose of Photofrin was 5 mg/kg and the irradiation parameters were 150 mW/cm^2 and 100 J/cm^2. This dose has been used in most of the reported Photofrin–PDT experiments on animal tumor models.[12-14]Because it has been reported that higher fluence rates lead to a greater depletion of oxygen during light delivery,[13,15,16]a fluence rate of 150 mW/cm^2 was used. In the human sarcoma xenograft model, Engbrecht et al.[17]noted that the total light fluence had dose-response relationship to Photofrin-mediated PDT. However, increasing mortality was observed with increasing total light fluences, and three of six mice died after light delivery at a fluence of 150 J/cm^2.[17] In the angiosarcoma model, which has some histopathologic features similar to hemangioma, significant tumor volume reduction and a clear histological changes were observed after light delivery at a fluence of $100J/cm^2$.[4,12] Because hemangiomas have a benign nature and never recur after regression, our study was carried out at a fluence of $100J/cm^2$. Light was delivered at 24 hours after Photofrin administration because this time interval has been used in other Photofrin-mediated PDT experiments in animal tumor models,[12,17] and confocal analysis demonstrated an effective accumulation of Photofrin in the hemangioma tissue at 24 hours after administration.

The mechanism of tumor responses to PDT include direct cytotoxic effect, vascular damage, and acute inflammatory or immune reaction.[18,19] A direct cytotoxic effect and vascular damage are initiating events to destroy a tumor cell.[19] Engbrecht et al.[17] noted that the mechanism of tumor destruction by PDT appears to be vascular damage with initial apoptosis in tumor endothelial cells and delayed tumor cell apoptosis because endothelial cell with its higher oxygen content and/or greater Photofrin level, are susceptible to PDT-induced apoptosis. Henderson and Dougherty[20] noted that the most easily and rapidly discernable acute effects of PDT *in vivo* are of a vascular nature. This finding implies that PDT may also have rapidly discernible acute effects on infantile hemangioma

because infantile hemangioma is a benign vascular tumor. In our results, at 2 weeks, most of the implant volume had decreased by approximately 72.6%, and the volume was significantly decreased in the treated implants compared with the untreated implants. At 12 hours after PDT, CD31 staining showed disruption of the endothelial lining, and apoptotic cells were commonly stained with the TUNEL method. At 24 hours after PDT, CD31 staining cell was rarely observed. These results showed that most of endothelial cells, which are the major components of hemagiomas, were destroyed by apoptosis within 24 hours. Because hemangiomas, due to their vascular nature, are more "angiogenesis dependent" than other tumors, relying on the recruitment of new blood vessels for their growth,[21] they might show more effective response to PDT.

The instantaneous vascular response caused by PDT, including vessel constriction, release of clotting factor, platelet aggregation and vascular collapse, lead to blood vessel occlusion, blood flow stasis, and hemorrhage,[19]and the subsequent ischemic condition can cause apoptosis. Because the histological features of our implants were identical to the proliferative phase, with a particularly high metabolic rate, and the endothelial cells, a major cellular component of the implant, responded to PDT immediately, the condition of acute ischemia was considered anoxia rather than hypoxia. Hypoxia–inducible factor-1α (HIF-1α) is one of the key enzymes in regulating gene expression after ischemia.[22,23] However, several studies noted that cells and tissue can respond to severe hypoxia or anoxia independent of HIF-1α signaling.[24,25] ATF3 is a transcription factor that was found to be induced in tumor cells under stress conditions, especially under anoxia.[26-28] The expression of ATF3 is ubiquitous, but it is maintained at a very low level in normoxia; however, it is induced quickly under severe hypoxia or anoxia.[29] Under these severe hypoxia or anoxia condition, ATF3 expression is up regulated in a wide variety of tissues such as heart, kidney, and brain.[30,31] Additionally, ATF3 is highly expressed in vascular endothelial cells in human atherosclerotic lesions and has been implicated in cell death.[32] Therefore, we investigated the change in ATF3 immediately after PDT(< 12 hours). ATF3 expression increased gradually and then reached a maximum level 4 hours after PDT, which was approximately 2-fold over baseline. Within 12 hours after PDT, ATF3-mediated pathway, which is involved in ischemia-induced apoptosis, was activated. Therefore, apoptosis, which is a

major mechanism of hemangioma destruction in the early phase, might be caused by ischemic injury as well as the direct cytotoxic effect of PDT.

Conclusion

We evaluated the efficacy of PDT against infantile hemangioma using an experimental model of xenografted human hemangioma tissue. The volumes were significantly decreased in PDT-treated hemangiomas compared with the untreated hemangiomas, and on histological examination, the significant destruction of endothelial cells, which are the main component of hemangiomas, was observed in the PDT-treated hemangiomas. Therefore, PDT can be considered as an alternative treatment for infantile hemangiomas when several clinical problems requiring pharmacologic and surgical treatments occur.

REFERENCES

1. Hidano A, Purwoko R, Jitsukawa K. Statistical survey of skin changes in Japanese neonates. *Pediatr Dermatol* 1986;3:140–4.

2. Jacobs AH, Walton RG. The incidence of birthmarks in the neonate. *Pediatrics* 1976;58: 218–22.

3. Barlow CF, Priebe CJ, Mulliken JB, et al. Spastic diplegia as a complication of interferon alfa-2a treatment of hemangioma of infancy. *J Pediatr* 1998;132:527-30.

4. Middelkamp-Hup MA, Sánchez-Carpintero I, Kossodo S, Waterman P, González S, Mihm MC Jr, Anderson RR. Photodynamic therapy for cutaneous proliferative vascular tumors in a mouse model. *J Invest Dermatol*2003;121:634-9.

5. Tang Y, Liu W, Yu S, Wang Y, Peng Q, Xiong Z, Wang Y, Wei T. A novel in vivo model of human hemangioma: xenograft of human hemangioma tissue on nude mice. *Plast Reconstr Surg* 2007;120:869-78.

6. Bi Y, Gao J, Yao M. Nude mice Wilm's tumor model. *Chin J Pediatr Surg* 2000;21:115-8.

7. Patterson MS, Wilson BC. Photodynamic therapy. In: Morden Technology of Radiation Oncology. Dyh JV (Ed.) Madison, Medical Physics Publishing, Madison (1999):941-980

8. North PE, Wander M, Mieracki A, Mihm MC Jr. GLUT1: a newly discovered immunohistochemical marker for juvenile hemangiomas. *Hum Pathol* 2000;31:11-22.

9. Leon-Villapalos J, Wolfe K, Kangesu L. GLUT-1: an extra diagnostic tool to differentiate between hemangiomas and vascular malformations. *Br J Plast Surg* 2005;59:348-52.

10. Leunig A, Staub F, Peters J, Heimann A, Csapo C, Kempski O, Goetz AE. Relation of early Photofrin uptake to photodynamically induced phototoxicity and changes of cell volume in diVerent cell lines. *Eur J Cancer* 1994;30:78–83.

11. Chamlin SL, Haggstrom AN, Drolet BA, Baselqa E, et al. Multicenter prospective study of ulcerated hemangiomas. *J Pediatr* 2007;151:684- 9.

12. Jin I, Yuji M, Yoshinori N, Makoto K, Mikio M. Anti-tumor effect of PDT using Photofrin in a mouse angiosarcoma model. *Arch Dermatol Res*2008;300:161-6.

13. Sitnik TM, Henderson BW. The effect of fluence rate on tumor and normal tissue responses to photodynamic therapy. *Photochem Photobiol* 1998;67:462–6.

14. Xiao Z, Brown K, Tulip J, Moore RB. Whole bladder photodynamic therapy for orthotopic superficial bladder cancer in rats: a study of intravenous and intravesical administration of photosensitizers. *J Urol* 2003;169:352–6.

15. Foster T H, Murant RS, Bryant RG, Knox RS, Gibson SL, Hilf R. Oxygen consumption and diffusion effects in photodynamic therapy. *Radiat Res*1991;126:296–303.

16. Robinson DJ, de Bruijn HS, van der Veen N, Stringer MR, et al. Fluorescence photobleaching of ALA-induced protoporphyrin IX during photodynamic therapy of normal hairless mouse skin: the effect of light dose and irradiance and the resulting biological effect. *Photochem Photobiol* 1998;67:140– 9.

17. Engbrecht BW, Menon C, Kachur AV, Hahn SM, Fraker DL. Photofrin-mediated photodynamic therapy induces vascular occlusion and apoptosis in a human sarcoma xenograft model. *Cancer Res* 1999;59:4334-42.

18. Buytaert E, Dewaele M, Agostinis P. Molecular effectors of multiple cell death pathways initiated by photodynamic therapy. *Biochim Biophys Acta* 2007;1776:86–107.

19. Firczuk M, Nowis D, Gołąb J. PDT-inducedinflammatory and hostresponses.*Photochem Photobiol Sci* 2011;10:653-63.

20. Henderson BW, Dougherty TJ. How does photodynamic therapy work? *Photochem Photobiol*1992;55:145–57.

21. Folkman J. Tumor angiogenesis: therapeutic implications. *N Engl J Med* 1971;285:1182-6.

22. Yee Koh M, Spivak-Kroizman TR, Powis G. HIF-1 regulation: Not so easy come, easy go. *Trends Biochem Sci* 2008;33:526–34.

23. Fong GH. Regulation of angiogenesis by oxygen sensing mechanisms. *J Mol Med* 2009;87:549–60.

24. Ameri K, Lewis CE, Raida M, Sowter H, Hai T, Harris AL. Anoxic induction of ATF-4 through HIF-1-independent pathways of protein stabilization in human cancer cells. *Blood* 2004;103:1876–82.

25. Blais JD, Filipenko V, Bi M, et al. Activating transcription factor 4 is translationally regulated by hypoxic stress. *Mol CellBiol* 2004;24:7469–82.

26. Ishiguro T, Nagawa H. Expression of the ATF3 gene on cell lines and surgically excised specimens. *Oncol Res* 2000;12:181–3.

27. Hai T, Wolfgang CD, Marsee DK, Allen AE, Sivaprasad U. ATF3 and stress responses. *Gene Expr* 1999;7:321–35.

28. Ameri K, Hammond EM, Culmsee C, Raida M, et al. Induction of activating transcription factor 3 by anoxia is independent of p53 and the hypoxic HIF signaling pathway. *Oncogene* 2007;26:284–9.

29.Wang L, Deng S, Lu Y, Zhang Y, Yang L, et al. Increased inflammation and brain injury after transient focal cerebral ischemia in activating transcription factor 3 knockout mice. *Neuroscience*2012;220:100–8.

30. Yin T, Sandhu G, Wolfgang CD, Burrier A, Webb RL, et al. Tissue-specific pattern of stress kinase activation in ischemic/reperfused heart and kidney. *J Biol Chem* 1997;272,19943–50.

31. Song DY, Oh KM, Lee JH, Woo RS, Lee YJ, et al. Expression of activating transcription factor 3 in ischemic penumbra region following focal cerebral ischemia. *Korean J Anat* 2008;41:173–83.

32.Nawa T, Nawa MT, Adachi MT, Uchimura I, et al. Expression of transcriptional repressor ATF3/LRF1 in human atherosclerosis: colocalization and possible involvement in cell death of vascular endothelial cells.*Artherosclerosis*2002 ;161:281-91.

국문초록

목 적: 저자들은 혈관종 동물모델을 이용하여 유아 혈관종에 대한 광역동학 치료의 효과를 조사하였다.

대상 및 방법: 5명으로부터 얻은 83개의 혈관종 조직을 누드 마우스에 이식하고, 그 형태와 부피의 변화를 최대 13주까지 관찰하였다. 시료 이식 5주 후 이식된 시료의 조직학적 변화를 관찰하고, 광역학동 치료를 이식 후 6에서 10주 사이에 시행하였다. 광민감제 주입 후 24시간 후에 이식물의 광민감제 흡수를 평가하였다. 빛을 조사한 후 0, 12, 24시간 후에 이식된 시료의 반응을 측정하였다. 또한 심각한 저 산소 환경에서 발현되는 전사 인자인 ATF3를 측정하였다.

결과: 이식된 시료의 부피는 첫 4주간 서서히 증가하였으나, 이후 퇴축하였다. 이식 5주째에 불룩한 내피세포가 밀집된 사인 곡선 형태의 채널을 형성하고 있음이 관찰되었으며, 그 혈관내피세포들은 CD31과 GLUT1에 양성이었다. 광민감제 투여 24시간 후에 공 초점 현미경 상 광민감제가 CD31양성인 세포 안에 나타나는 것이 관찰되었다. 이식물의 부피는 광역동학 치료 후 대조군에 비해 유의하게 감소하였다 ($p < .0001$). 빛 조사 24시간 후에 대부분의 세포들은 붕괴되었다. ATF3의 발현은 치료 후 점진적으로 증가하여 4시간 후에 최대치에 도달하였다.

결론: 광역동학 치료는 유아 혈관종 치료에 효과적이었다. 세포사멸이 유아 혈관종 치료 효과의 주요 기전이며, 광역동학 치료의 직접적인 효과 뿐만 아니라 허혈 손상에 의해 유발되는 것으로 생각된다.

색인 단어: 광영동학 치료, 혈관종 동물모델,포토프린(photofrin), 글루트1(GLUT1), 에이티에프3(ATF3), 혈관내피 세포
학번: 2005-30606